

# Quater-, Quinque-, and Sexithiophene Organogelators: Unique Thermochromism and Heating-Free Sol–Gel Phase Transition

Shin-ichiro Kawano, Norifumi Fujita, and Seiji Shinkai\*<sup>[a]</sup>

**Abstract:** A series of quater-, quinque-, and sexithiophene derivatives bearing two cholesteryl groups at the  $\alpha$ -position, which are abbreviated as **4T-(chol)<sub>2</sub>**, **5T-(chol)<sub>2</sub>**, and **6T-(chol)<sub>2</sub>**, respectively, have been synthesized. It has been found that these oligothiophene derivatives act as excellent organogelators for various organic fluids and show the unique thermochromic behaviors through the sol–gel phase transition. It was shown on the basis of extensive investigations, performed with UV-visible spectroscopy, circular dichroism (CD), transmission electron microscopy (TEM), scanning electron microscopy (SEM), and atomic force

microscopy (AFM), that these gelators self-assemble into the one-dimensional structures in the organogels, in which the  $\pi$ -block moieties of the oligothiophenes are stacked in an H-aggregation mode. Surprisingly, an AFM image shows that **4T-(chol)<sub>2</sub>** forms unimolecular fibers in a left-handed helical sense, whereby one pitch of the helical fiber is constructed by 400–540 **4T-(chol)<sub>2</sub>** molecules. Very interestingly,

the conformational change in the oligothiophene moieties can be visually detected: for example, **6T-(chol)<sub>2</sub>** shows a specific absorption maximum in the gel ( $\lambda_{\text{max}} = 389 \text{ nm}$ ) and in the solution ( $\lambda_{\text{max}} = 439 \text{ nm}$ ). In addition, a sol–gel phase transition of the **6T-(chol)<sub>2</sub>** gel was implemented by addition of oxidizing and reducing reagents such as  $\text{FeCl}_3$  and ascorbic acid, respectively. The stimuli-responsive functionality of the oligothiophene-based organogels makes them promising candidates for switchable opto- and electronic soft materials.

**Keywords:** nanostructures • oligothiophenes • sol–gel processes • supramolecular chemistry • thermochromism

## Introduction

Effective conjugation length is an index expressing the  $\pi$ -electronic nature of  $\pi$ -conjugated organic molecules that now play a central role of materials chemistry. In case of thiophene sequences in oligo- and polythiophenes, the effective conjugation length is mainly governed by *anti* versus *syn* conformations of thiophene rings.<sup>[1]</sup> However, although the *anti* conformation of the thiophene sequences is thermodynamically more favorable than that of the *syn* conformation, effective conjugation length becomes rather short in solution because oligothiophenes enjoy a dynamic rotation of thiophene rings. Even in the solid state such as thin films,

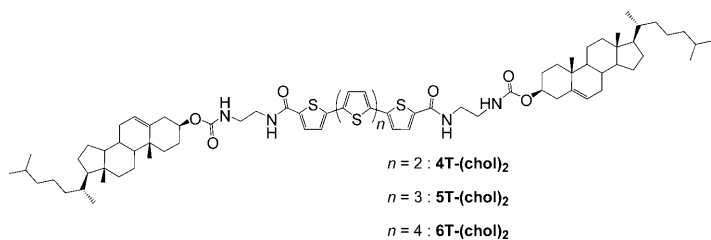
*syn-anti* mixing in thiophene sequences often causes polymorphism leading to the serious lack of the physical properties characteristic of these  $\pi$ -conjugation systems.<sup>[2]</sup>

Recently,  $\pi$ -block-based low-molecular-weight gels have occupied the attention of supramolecular chemists, because these one-dimensional objects inspire construction of novel energy-transfer systems and nanowire-based devices.<sup>[3]</sup> In such integrated systems,  $\pi$  blocks should interact with each other through  $\pi$ – $\pi$  interactions in the self-assembled architectures; a requirement for this is that the  $\pi$ -conjugated sequence needs to be as planar as possible and the *anti* conformation should be favored. In this context, we have demonstrated an effective molecular design strategy for organogelators, in which  $\pi$  blocks are covalently linked together and contain a cholesteryl group at each end.<sup>[4]</sup> The  $\pi$ – $\pi$  stacking between the  $\pi$  blocks and van der Waals forces between the cholesteryl groups cooperatively work, leading to formation of stable gels in various organic fluids. In addition, these gelators often offer high transparency that enables us to readily investigate optical properties of these gels. Herein, we report oligothiophene-based gelators bearing cholesteryl groups at both ends of the thiophene sequences (**4T-(chol)<sub>2</sub>**,

[a] S.-i. Kawano, Dr. N. Fujita, Prof. Dr. S. Shinkai  
Department of Chemistry & Biochemistry  
Graduate School of Engineering, Kyushu University  
6-10-1 Hakozaki, Higashi-ku, Fukuoka 812-8581 (Japan)  
Fax: (+81)92-642-3611  
E-mail: seijitem@mbox.nc.kyushu-u.ac.jp

Supporting information for this article is available on the WWW under <http://www.chemeurj.org/> or from the author.

**5T-(chol)<sub>2</sub>** and **6T-(chol)<sub>2</sub>**, expecting that *anti* oligothiophene cores should stack through strong  $\pi$ - $\pi$  interactions in the gel phase and the resultant gel systems should have new physical and chemical properties.<sup>[5]</sup>



To design these oligothiophene-based gelators, we took the following points into consideration:

- 1) Their reversible sol-gel phase-transition behavior between the solution and the gel should induce significant transformation of effective conjugation length (Figure 1).

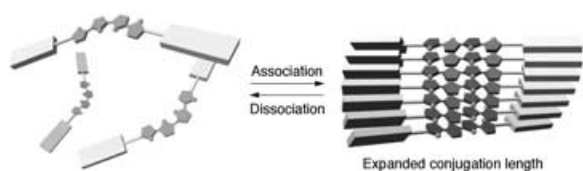


Figure 1. Schematic representation of a chromatic change accompanied with self-assembly.

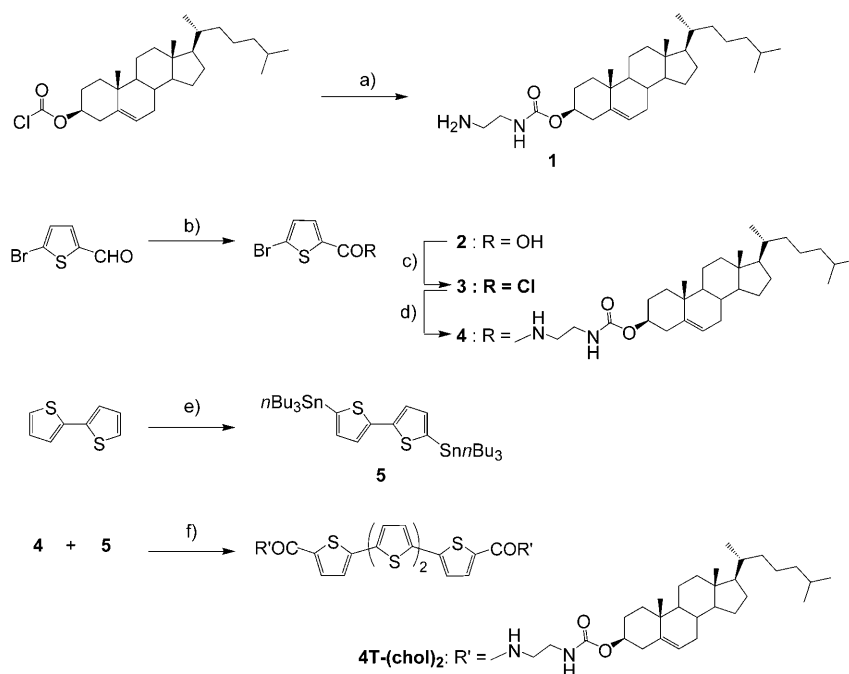
- 2) Oligothiophene derivatives consisting of more than quaterthiophene sequence possess strong absorption bands in visible region leading to a dramatic color change when they are coupled with the sol-gel phase transition
- 3) Oligothiophene moieties can be easily oxidized to form radical cation species, leading to electrostatically repulsive disintegration of the gelators and resulting in the reversible sol-gel phase control.<sup>[4b,6,7]</sup>

Although Feringa et al. already reported the investigation on thiophene- or bithiophene-based organogelators,<sup>[8]</sup> the authors mainly focused on the conductivities of the gels and did not evaluate the gela-

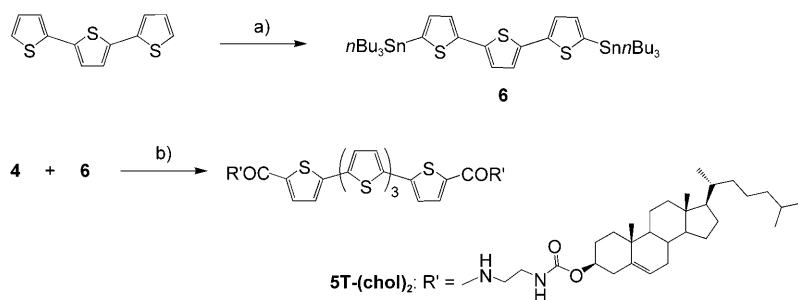
tors in the view of the chromophore, which can be regulated by the conformational change in the  $\pi$ -conjugation system. For the present system, as well as extensive spectrometric analyses, we have investigated the unique chromatic properties of the longer oligothiophene-based gelators, which are controlled with the sol-gel phase-transition.

## Results and Discussion

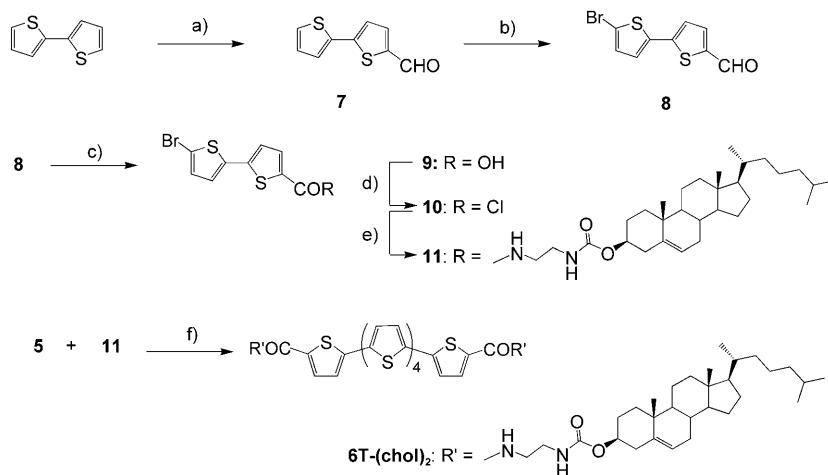
**Syntheses of oligothiophene-based gelators:** Each step of the synthetic procedures of **4T-(chol)<sub>2</sub>**-**6T-(chol)<sub>2</sub>** was based on literature methods previously reported.<sup>[9-11]</sup> This entails a straightforward coupling reaction of cholesterol-attached mono- or bithiophene derivatives with oligothiophene cores to give the desired molecules (Schemes 1-3). 3 $\beta$ -Cholest-5-en-3-yl-*N*-(2-aminoethyl) carbamate (**1**),<sup>[9]</sup> 5-bromo-2-thiophenecarboxylic acid (**2**),<sup>[10]</sup> 5,5'-bis[tris(*n*-butyl)stannyl]-2,2'-bithiophene (**5**),<sup>[10]</sup> 2,2'-bithiophene-5-carboxaldehyde (**7**),<sup>[11]</sup> and 5-bromo-2,2'-bithiophene-5'-carboxaldehyde (**8**),<sup>[11]</sup> and the acid analogue (**9**)<sup>[10]</sup> were prepared according to the literatures reported previously. The acid chlorides **3** and **10** were prepared according to a standard reaction with SOCl<sub>2</sub>. These compounds were characterized by IR and <sup>1</sup>H NMR spectroscopy and used for the following key steps. Differing from the most cases in the final step of the syntheses of gelator molecules, appropriate selection of the solvent and the proper concentration for the Stille coupling reaction enabled us to avoid the reaction system from becoming viscous. As a result, **4T-(chol)<sub>2</sub>**-**6T-(chol)<sub>2</sub>** were successfully obtained in practical yields from **4** + **5**, **4** + **6**, and **5** + **11** simply by repre-



Scheme 1. Synthesis of oligothiophene-based gelator **4T-(chol)<sub>2</sub>**. a) Ethylenediamine, CH<sub>2</sub>Cl<sub>2</sub>, 0-20 °C, 4 h; b) NaClO<sub>2</sub>, H<sub>2</sub>O<sub>2</sub>, CH<sub>3</sub>CN, and H<sub>2</sub>O, 10 °C, 1 h; c) SOCl<sub>2</sub>, 80 °C, 4 h; d) **1**, triethylamine, CH<sub>2</sub>Cl<sub>2</sub>, 0-20 °C, 3.5 h; e) *n*BuLi, *n*Bu<sub>3</sub>SnCl, diethyl ether, 20 °C, 12 h; f) [Pd(PPh<sub>3</sub>)<sub>2</sub>Cl<sub>2</sub>], DMF, 80 °C, 12 h.



Scheme 2. Synthesis of oligothiophene-based gelator **5T-(chol)<sub>2</sub>**, a) *n*BuLi, *n*Bu<sub>3</sub>SnCl, diethyl ether, 20 °C, 12 h; b) [Pd(PPh<sub>3</sub>)<sub>2</sub>Cl<sub>2</sub>], DMF, 80 °C, 12 h.



Scheme 3. Synthesis of oligothiophene-based gelator **6T-(chol)<sub>2</sub>**, a) POCl<sub>3</sub>, DMF, 1,2-dichloroethane, 60 °C, 4 h; b) Br<sub>2</sub>, NaHCO<sub>3</sub>, CHCl<sub>3</sub>, 70 °C, 4 h; c) NaClO<sub>2</sub>, H<sub>2</sub>O<sub>2</sub>, CH<sub>3</sub>CN, and H<sub>2</sub>O, 10 °C, 1 h; d) SOCl<sub>2</sub>, 80 °C, 4 h; e) 1, triethylamine, CH<sub>2</sub>Cl<sub>2</sub>, 0–20 °C, 3.5 h; f) [Pd(PPh<sub>3</sub>)<sub>2</sub>Cl<sub>2</sub>], DMF, 80 °C, 12 h.

precipitation. The final products were characterized by <sup>1</sup>H NMR spectroscopy, MALDI-TOF-MS, and elemental analyses.

**Gelation properties of 4T-(chol)<sub>2</sub>–6T-(chol)<sub>2</sub>:** The gelation properties of oligothiophene derivatives **4T-(chol)<sub>2</sub>–6T-(chol)<sub>2</sub>** were evaluated in various solvents (Table 1). Derivatives **4T-(chol)<sub>2</sub>** and **5T-(chol)<sub>2</sub>** gelled various kinds of non-polar solvents such as benzene, toluene, benzonitrile, 1,1,2,2-tetrachloroethane (TCE), and Decalin as well as a few kinds of polar solvents such as THF, DMSO, and so forth. In many cases, the gels showed high transparency and stability even at concentrations as low as 1.5 mM. In contrast, **6T-(chol)<sub>2</sub>** was insoluble in most common solvents tested and gelled only five solvents, that is, anisole, benzonitrile, diphenyl ether, TCE, and pyridine. The insolubility of **6T-(chol)<sub>2</sub>** is ascribed to the strong π–π interaction between the sexithiophene moieties. Derivative **6T-(chol)<sub>2</sub>** had a high propensity to aggregate by itself in these concentration region. This problem is discussed more in detail in a later section.

**TEM and SEM investigations:** To obtain visual images of the **4T-(chol)<sub>2</sub>–6T-(chol)<sub>2</sub>** aggregates in the gels we took pic-

tures with transmission and scanning electron microscopes (TEM and SEM; Figure 2). One can consistently observe well-developed network structures composed of fibrous aggregates. Moreover, these gels have a high aspect ratio of the fibers, in which the length is more than several micrometers and the diameters are 7–20 nm. In the TEM image of the **4T-(chol)<sub>2</sub>** gel, the shortest diameter of the fiber is about 7 nm, which is comparable with the molecular long axis of **4T-(chol)<sub>2</sub>** (6.6 nm). In the SEM image of the **4T-(chol)<sub>2</sub>** gel, one can clearly recognize a left-handed helical motif (Figure 2b, inset). This helical motif is consistent with the model expected in the Figure 1 and also supported by the negative exciton coupling (*S* chirality) obtained from the CD measurements (vide infra). It was also found that **5T-(chol)<sub>2</sub>** and **6T-(chol)<sub>2</sub>** gels form the three-dimensional fibrous networks in organic fluids (Fig-

Table 1. Gelation properties of **4T-(chol)<sub>2</sub>**, **5T-(chol)<sub>2</sub>**, and **6T-(chol)<sub>2</sub>** at 25 °C.<sup>[a–c]</sup>

Solvent	<b>4T-(chol)<sub>2</sub></b>	<b>5T-(chol)<sub>2</sub></b>	<b>6T-(chol)<sub>2</sub></b>
benzene	G (2.0)	G (2.5)	I <sup>---</sup>
toluene	G (2.0)	G (2.5)	I <sup>---</sup>
<i>p</i> -xylene	G (2.0)	G (2.2)	I <sup>---</sup>
diphenyl ether	G (2.0)	G (1.7)	G (2.0)
anisole	G (5.0)	G (1.7)	G (2.9)
benzonitrile	G (7.5)	G (3.3)	G (3.3)
TCE	G (2.0)	G (3.3)	G (5.0)
chloroform	G (2.1)	S <sup>+</sup>	I <sup>---</sup>
decalin	G (3.3)	G (5.0)	I <sup>---</sup>
cyclohexane	I	G (10)	I <sup>---</sup>
hexane	I	I <sup>---</sup>	I <sup>---</sup>
acetonitrile	I	I <sup>---</sup>	I <sup>---</sup>
1-butyronitrile	I	I <sup>---</sup>	I <sup>---</sup>
acetone	I	I <sup>---</sup>	I <sup>---</sup>
ethyl acetate	I	I <sup>---</sup>	I <sup>---</sup>
THF	G (7.5)	G (5.0)	I <sup>---</sup>
1-octanol	G (2.0)	G (2.9)	S <sup>---</sup>
1-butanol	I <sup>---</sup>	I <sup>---</sup>	I <sup>---</sup>
ethanol	I	I <sup>---</sup>	I <sup>---</sup>
pyridine	S <sup>+</sup>	G (10)	G (6.7)
DMSO	G (15)	P <sup>++</sup>	I <sup>---</sup>
DMF	G (15)	P <sup>++</sup>	P <sup>-</sup>

[a] X<sup>++</sup>, X<sup>+</sup>, X, X<sup>-</sup>, X<sup>---</sup>, and X<sup>----</sup> denote the concentrations of 10, 5.0, 4.0, 3.3, 2.5, and 2.0 g dm<sup>-3</sup>, respectively. [b] G: gel, P: precipitation, S: solution, and I: insoluble when heated. [c] The critical gelation concentrations [g dm<sup>-3</sup>] of gelators are shown in the parentheses.

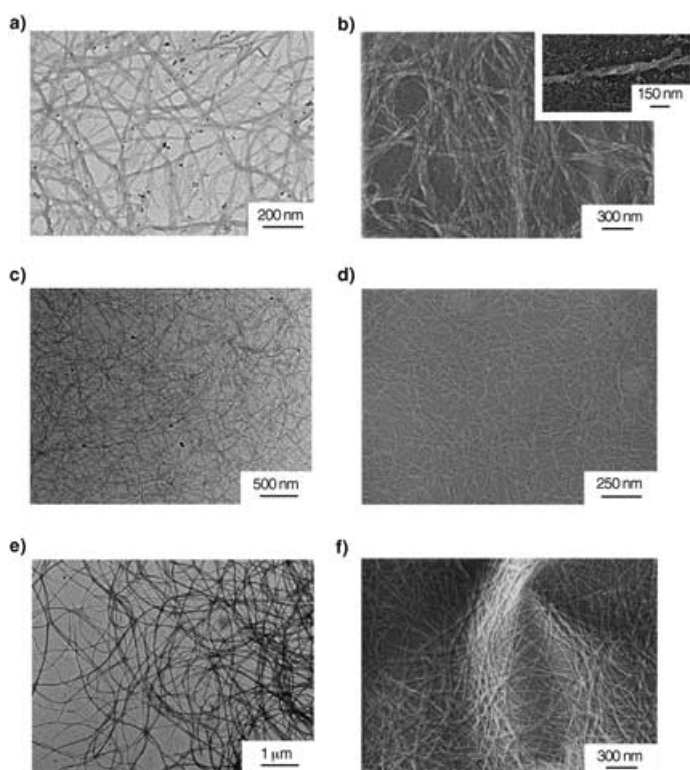


Figure 2. TEM (left) and SEM (right) images of xerogels prepared from **4T-(chol)<sub>2</sub>** (top), **5T-(chol)<sub>2</sub>** (middle), and **6T-(chol)<sub>2</sub>** (bottom) gels. Conditions: a) [**4T-(chol)<sub>2</sub>**]=1.5 mm in TCE, b) [**4T-(chol)<sub>2</sub>**]=1.0 mm in toluene, c) and d) [**5T-(chol)<sub>2</sub>**]=2.9 mm in TCE, e) and f) [**6T-(chol)<sub>2</sub>**]=3.8 mm in TCE.

ure 2c–f). The high aspect ratio of the fibers composed of oligothiophene derivatives is certainly reminiscent of a functional nanowire.

**AFM investigations:** More surprisingly, AFM observation offered important evidence of unimolecular helical aggregates of **4T-(chol)<sub>2</sub>** (Figure 3a). Detailed examination of this image revealed that the height of the fibrous aggregate is approximately 6.8–7.3 nm (Figure 3b), which is consistent with the molecular long axis of **4T-(chol)<sub>2</sub>**. Furthermore, it was again confirmed that the fibrous aggregate of **4T-(chol)<sub>2</sub>**

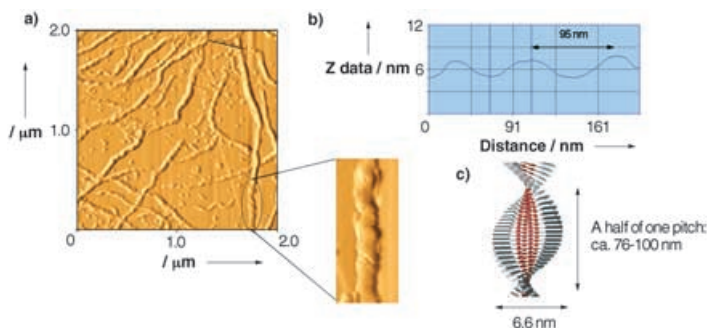


Figure 3. a) AFM image of **4T-(chol)<sub>2</sub>** (1.0 mm in TCE), b) the height profile along the solid line in Figure 3a, and c) schematic illustration of the helical fiber of **4T-(chol)<sub>2</sub>**.

adopts a left-handed helical motif along its one-dimensional aggregate. In the height profile of the fibers (Figure 3b), the periodic top-to-top length of the helical structure is about 76–100 nm. This length corresponds to half of the helical pitch (Figure 3c). As the distance between the  $\pi$ -stacked oligothiophene moieties can be estimated to be about 0.38 nm,<sup>[12]</sup> one can consider that this half of one pitch is constructed by 200–270 **4T-(chol)<sub>2</sub>** molecules.

**Variable-temperature <sup>1</sup>H NMR studies:** Variable-temperature <sup>1</sup>H NMR studies showed that the peak signals assignable to the urethane and amide NH protons of **4T-(chol)<sub>2</sub>** are more downfield shifted at room temperature in 1,1,2,2- $C_2D_2Cl_4$  (1.0 mm) than those at 100 °C ( $\Delta\delta=0.40$  and 0.15 ppm, respectively). The finding clearly indicates that formation of the intermolecular hydrogen bonds also contributes to the aggregation of **4T-(chol)<sub>2</sub>**. These results are well compatible with the aggregation model proposed for **4T-(chol)<sub>2</sub>** (Figure 1). However, the detailed analyses of the <sup>1</sup>H NMR spectra were difficult because of the significant line broadening, particularly in the gel phase.

**UV-visible and CD spectroscopic analyses:** Interestingly, reversible thermochromic behavior was observed for **4T-(chol)<sub>2</sub>**–**6T-(chol)<sub>2</sub>** through the sol–gel phase transition (Figure 4). For example, when the orange **4T-(chol)<sub>2</sub>** gel was

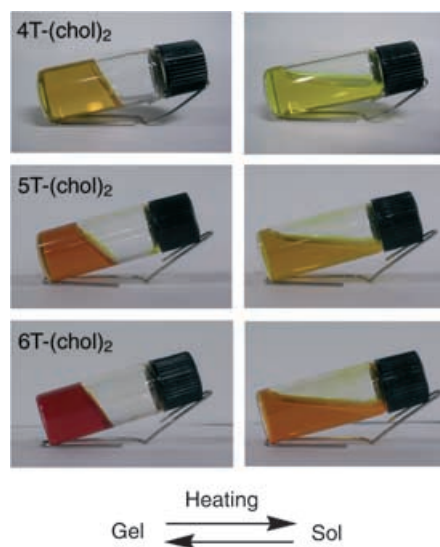


Figure 4. Phase transition and thermochromic behavior of the sol (right) and gel (left) phases prepared from **4T-(chol)<sub>2</sub>**, **5T-(chol)<sub>2</sub>**, and **6T-(chol)<sub>2</sub>** in TCE.

heated, a yellow solution was produced. To the best of our knowledge, there is no preceding example that such a clear color change can be induced by a conformational change of the  $\pi$ -conjugation system. Hence, we measured the absorption spectra of this gel at various temperatures to elucidate the origin of this color change. As shown in Figure 5a, a spectrum of the **4T-(chol)<sub>2</sub>** gel with TCE (20 °C) showed a

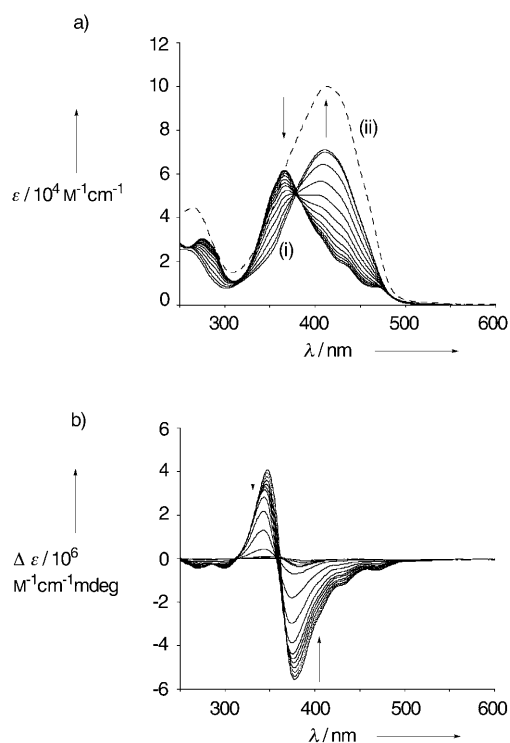


Figure 5. Temperature dependence of a) absorption and b) CD spectra of **4T-(chol)<sub>2</sub>** gel in TCE: i) [**4T-(chol)<sub>2</sub>**]<sub>gel</sub> = 1.5 mm, 20 to 80 °C (red to blue) and ii) a dotted line in Figure 5a shows a spectrum of the solution ([**4T-(chol)<sub>2</sub>**]<sub>sol</sub> = 20 μM, 20 °C).

$\pi$ - $\pi$  transition band at 367 nm, whereas a spectrum of the dilute solution **4T-(chol)<sub>2</sub>** in TCE (20 °C) had the absorption maximum at 418 nm. Moreover, the  $\pi$ - $\pi$  transition band of the **4T-(chol)<sub>2</sub>** gel significantly decreased and the absorbance at 411 nm, which was assigned to the nonaggregated **4T-(chol)<sub>2</sub>**, gradually appeared when the temperature was raised to 80 °C.<sup>[13]</sup> These results can be explained as formation of an H-aggregate from **4T-(chol)<sub>2</sub>** by means of a molecular exciton model, assuming a parallel orientation of oligothiophene moieties.<sup>[14]</sup> In addition, appearance of vibrational fine structures (shoulder bands at  $\lambda$  = 408, 434, and 467 nm) was also confirmed in the gel phase. These results indicate an increase in the effective conjugation length as well as an increase in the conformational order in the aggregates.<sup>[15]</sup> Raman spectral measurements of the **4T-(chol)<sub>2</sub>** sol and the gel in TCE also supported this proposal. Thienyl groups have characteristic Raman bands in 1550–1000  $\text{cm}^{-1}$  spectral region. The sol phase of **4T-(chol)<sub>2</sub>** at 0.15 mm showed four bands at 1550–1500  $\text{cm}^{-1}$  attributed to the in-phase C=C antisymmetric vibration. On the other hand, the gel phase at 2.0 mm had only one band in this region. In addition, the intensity of this band was weakened relative to the strongest  $\nu(\text{C}=\text{C})$  band at 1461  $\text{cm}^{-1}$ , more than that in the sol phase (see Supporting Information). The results indicate that the thienyl moieties in the gel phase adopt an *anti*-rich conformation and have a simpler distribution among several possible conformations than that in the sol phase.<sup>[16]</sup> It is likely from these results, therefore, that the quaterthio-

phene moieties are  $\pi$ -stacked and adopt an H-aggregation mode in the gel phase, similar to rigid  $\pi$ -systems (e.g., perylene) in the organogel phase.<sup>[4a]</sup>

In addition, the **4T-(chol)<sub>2</sub>** gel showed a temperature-dependent, strong negative Cotton effect in the  $\pi$ - $\pi^*$  transition band region with the  $\theta=0$  crossing wavelength near the absorption maximum (367 nm) in the CD spectra (Figure 5b). It was confirmed that the contribution of linear dichroism to these spectra is negligible. These results indicate that the chromophores of the quaterthiophene moieties of **4T-(chol)<sub>2</sub>** self-assemble in a helical sense and the dipole moments are oriented in an anticlockwise direction.<sup>[17]</sup> The results are in accord with the morphological observation by SEM and AFM. Derivatives **5T-(chol)<sub>2</sub>** and **6T-(chol)<sub>2</sub>** show the similar behavior to that of **4T-(chol)<sub>2</sub>** in the UV-visible absorption and CD experiments (see Table 2 and Supporting Information).

Table 2. Absorption maxima of the aggregated species ( $\lambda_{\text{agg}}$ ), the absorption maxima of the nonaggregated species ( $\lambda_{\text{free}}$ ), and binding constants  $K$  of **4T-(chol)<sub>2</sub>**, **5T-(chol)<sub>2</sub>**, and **6T-(chol)<sub>2</sub>** in TCE.

Gelator	$\lambda_{\text{agg}}$ [nm]	$\lambda_{\text{free}}$ [nm]	$K$ [ $\text{L}\cdot\text{mol}^{-1}$ ]
<b>4T-(chol)<sub>2</sub></b>	367	419	$0.5 \times 10^3$
<b>5T-(chol)<sub>2</sub></b>	370	424	$2.2 \times 10^4$
<b>6T-(chol)<sub>2</sub></b>	388	439	$2.7 \times 10^5$

These findings consistently support the view that the conformation of the oligothiophene moieties is drastically changed to facilitate the  $\pi$ - $\pi$  stacking in the gel phase, which is sensitively reflected by the color change.

#### Sol-gel phase transition of the **6T-(chol)<sub>2</sub>** gel by redox stimuli

One of the most promising properties that organogels can offer is a stimulated response leading to the reversible sol-gel phase transition.<sup>[18]</sup> Although various types of the stimuli have been applied so far, a redox stimulus is important for the construction of the electromechanical soft materials, such as artificial muscles, electrorheological fluids, and so forth.<sup>[6]</sup> When a 1.0 molar equivalent of  $\text{FeCl}_3$  was added to a **6T-(chol)<sub>2</sub>** gel in TCE (4.0 mm) as an oxidizing reagent and the mixture was vigorously stirred for two minutes, the red gel turned into the dark-brown solution.<sup>[19]</sup> Then a 1.2 molar equivalent of ascorbic acid (AsA) was added to this solution as a reducing reagent and the mixture was left without heating. After one hour, the red gel was reproduced (Figure 6). It should be emphasized that this sol-gel phase transition can be attained simply by adding the chemicals

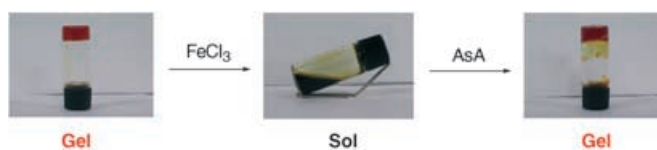


Figure 6. Sol-gel phase transition of the **6T-(chol)<sub>2</sub>** gel in TCE triggered by chemical oxidation and reduction.

without any heating–cooling process: in general, the gel is regenerated only by heating the sol above the sol–gel phase transition temperature. The oxidized sample shows the ESR-active species attributed to radical cation generation in the sexithiophene derivative (see Supporting Information). We believe, therefore, that this is a unique example of a heating-free sol–gel phase transition attained by combination with the redox reaction of **6T-(chol)<sub>2</sub>**. We consider that this property is related to the nature of the unimolecular fiber structure: even in the sol phase, short fibrous pieces do not precipitate and easily reconstruct the long fibers capable of suppressing solvent fluidity.

**The aggregation tendency of the oligothiophene-based organogels:** Although a lot of organogelators have already been reported thus far, most of the organogels have been accidentally produced. That is the reason why numerical principles for designing effective organogelators have been long-awaited. In this context, the aggregation tendency and binding constants of these  $\pi$ -block molecules, the concept of which was introduced by Martin,<sup>[20]</sup> have been evaluated by applying the equal- $K$  model to this one-dimensional self-assembled system.<sup>[21]</sup> The model assumes equal binding constants for all binding events in a one-dimensional columnar aggregate of a homo species, which is driven by the  $\pi$  stacking of aromatic moieties. The present oligothiophene-based organogels well-suit this model because 1) these organogels offer the one-dimensional unimolecular aggregates, directly supported by TEM and AFM investigations, and 2) one can distinguish the aggregated species from the nonaggregated in the concentration-dependent UV-visible absorption spectra (Table 2 and Supporting Information), which are similar to those in the temperature-dependent UV-visible absorption spectra (Figure 5a). Thus, as the present oligothiophene-based gelators exactly meet the requirements, this system is suitable for testing Martin's theory through systematic correlation between the gelation property and the aggregation tendency, focusing on the difference of the oligothiophene moieties. From the concentration-dependent UV-visible analyses, it has become clear that the longer the oligothiophene moieties are, the larger the binding constants are by one order of magnitude (Figure 7). For example, **6T-**

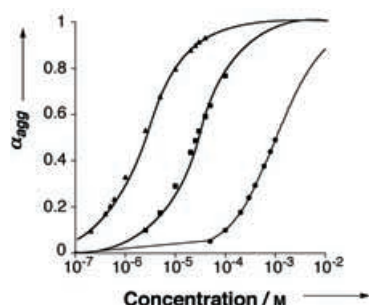


Figure 7. Concentration dependence of the molar ratio of the aggregate ( $\alpha_{\text{agg}}$ ) on **4T-(chol)<sub>2</sub>** (●), **5T-(chol)<sub>2</sub>** (■), and **6T-(chol)<sub>2</sub>** (▲) in TCE: for the method to determine  $\alpha_{\text{agg}}$ , see reference [21a].

**(chol)<sub>2</sub>** ( $K=2.7\times 10^5\text{M}^{-1}$ ) tends to self-assemble five hundreds times more effectively than **4T-(chol)<sub>2</sub>** ( $K=0.5\times 10^3\text{M}^{-1}$ ). These results show, therefore, that most of **6T-(chol)<sub>2</sub>** should be integrated in the aggregate at the concentration lower than the sol–gel phase-transition concentration. As mentioned in the gelation test section, **6T-(chol)<sub>2</sub>** has poor gelation properties relative to those of **4T-(chol)<sub>2</sub>** and **5T-(chol)<sub>2</sub>**. Therefore, the aggregation tendency of **6T-(chol)<sub>2</sub>** might be too strong to form an organogel ( $K\approx 10^5\text{M}^{-1}$ ). In other words, good gelators should have an adequate aggregation tendency ( $K\approx 10^3\text{--}10^4\text{M}^{-1}$ ), as long as the aggregation obeys the equal- $K$  model. We presume that a much stronger growth toward the one-dimensional direction of **6T-(chol)<sub>2</sub>** might lose the curvature of the fibers, leading to crystallization or precipitation by means of rapid bundling of fibrous aggregates.

## Conclusion

In conclusion, we have proposed that the  $\pi$ -conjugation length of thiophene sequences can be controlled under the self-assembled circumstances through the sol–gel phase transition; this results in the construction of the novel thermochromic organogels. According to this concept, we have successfully demonstrated that chromatic changes can influence a broad range of the spectra, in which the color of the samples can be changed from yellow to red. In addition, the redox active oligothiophene system has made the design of heating-free sol–gel phase control possible. Bearing this concept and results in our minds, this methodology can be applicable, more in general, to construction of other stimuli-responsive soft materials triggered by electro- or photochemical signals.

## Experimental Section

**General:** All chemical reagents were obtained from Aldrich, TCI, KISHIDA CHEMICAL or Wako were used without further purification. Dichloromethane was distilled over  $\text{CaH}_2$ . 1,2-Dichloroethane purchased from KISHIDA CHEMICAL was used. Distilled *N,N*-dimethylformamide was used. Diethyl ether and acetonitrile purchased from Wako were used as received unless otherwise noted.  $^1\text{H}$  NMR spectra were measured on Bruker AC-250PC and DMX 600 spectrometers. ATR-IR spectra were obtained using a Perkin–Elmer instrument Spectrum One FT-IR spectrometer. Mass spectral data were obtained using a Perseptive Voyager RP MALDI TOF mass spectrometer. UV/Vis, CD, ESR, and Raman spectra were measured on a Shimadzu UV-2500PC spectrometer, a Jasco J-720WI spectrometer, a JOEL JES-FE1XG ESR spectrometer, and a Perkin–Elmer System 2000 FT-Raman spectrometer, respectively.

**Gelation test of organic fluids:** The gelators and the solvents were put in a septum-capped test tube and heated until the solid was dissolved. The sample vial was cooled to 25 °C and left for 2 h at the ambient conditions. The state was evaluated by the “stable to inversion of a test tube” method.

**TEM and SEM measurements:** The gel was put on a carbon-coated copper grid and dried in vacuo for 12 h at room temperature. Then, the xerogel sample was subjected to TEM observations with a JEOL JEM-2010, operating at 120 kV. For SEM observations, the xerogels were

shielded by Pt and examined with a Hitachi S-5000 scanning electron microscope. The accelerating voltage of SEM was 15 kV.

**AFM measurements:** The **4T-(chol)<sub>2</sub>** gel was cast on a freshly cleaved highly oriented pyrolytic graphite (HOPG) with spin-coating (2000 rpm, 60 s). The sample was examined by Topometrix TMX-1010 (non-contact mode).

**Preparation of 3:** Compound **2** (2.6 g, 13 mmol) was added to SOCl<sub>2</sub> (46 mL, 0.63 mol) and the mixture was refluxed under nitrogen for 3 h. The excess SOCl<sub>2</sub> was evaporated under reduced pressure, and the resultant red oil was subjected to the next reaction.

**Preparation of 4:** A solution of **3** (2.8 g, 13 mmol) in CH<sub>2</sub>Cl<sub>2</sub> (50 mL) was added dropwise over a period of 2 h to a solution of **1** (6.0 g, 13 mmol) and triethyl amine (2.1 mL, 15 mmol) in CH<sub>2</sub>Cl<sub>2</sub> (50 mL) at 0 °C, and the reaction mixture was stirred at room temperature for 3.5 h. The solvent was removed by evaporation and the residue was purified by column chromatography (SiO<sub>2</sub>; CHCl<sub>3</sub>/AcOEt = 10:1) to give **4** (5.1 g, 7.7 mmol, 60%) as a yellow solid. M.p. 176–177 °C; <sup>1</sup>H NMR (250 MHz, CDCl<sub>3</sub>, 298 K): δ = 0.68 (s, 3H; CH<sub>3</sub>), 0.86–2.30 (m, 34H; CH, CH<sub>2</sub>, CH<sub>3</sub>), 3.42–3.43 (m, 2H; CH<sub>2</sub>), 3.51–3.52 (m, 2H; CH<sub>2</sub>), 4.47–4.48 (m, 1H; CH), 5.08–5.09 (m, 1H; NH), 5.35–5.36 (m, 1H; CH), 7.03 (d, *J* = 4.1 Hz, 1H; Ar), 7.15–7.16 (br, 1H; NH), 7.26 ppm (d, *J* = 4.1 Hz, 1H; Ar); ATR-IR: ν = 3314, 1723, 1697, 1625, 1572 cm<sup>-1</sup>; MS (MALDI-TOF, matrix; dithranol): 685.28 [M+Na]<sup>+</sup> (calcd: 684.77); elemental analysis calcd (%) for C<sub>35</sub>H<sub>53</sub>BrN<sub>2</sub>O<sub>3</sub>S: C 63.52, H 8.07, N 4.23; found: C 63.46, H 8.07, N 4.31.

**Preparation of 5:** A solution of 2,2'-bithiophene (0.38 g, 2.3 mmol) in diethyl ether (50 mL) was added dropwise over a period of 2 h to a solution of 15% *n*BuLi (15% in hexane; 3.4 mL) in diethyl ether (20 mL) at 0 °C under N<sub>2</sub>. Then the reaction mixture was stirred at room temperature for 1 h. The reaction mixture was then cooled to 0 °C. Tri-*n*-butyltin chloride (1.3 mL, 4.8 mmol) was added to the solution and the reaction mixture was stirred at room temperature for 12 h. The solvent was removed under reduced pressure and then the residue was subjected to the next step without further purification.

**Preparation of 4T-(chol)<sub>2</sub>:** A three-necked round bottom flask was charged with **4** (3.0 g, 4.5 mmol) and **5** (1.7 g, 2.3 mmol). The reagents were dissolved in distilled DMF (100 mL), and the solution was deaerated under vacuum and backfilled with argon ten times prior to the addition of the [Pd(PPh<sub>3</sub>)<sub>2</sub>Cl<sub>2</sub>] (0.08 g, 0.11 mmol). The reaction mixture was stirred for 12 h at 80 °C. The reaction was quenched with methanol, and the orange precipitate was filtered and washed with methanol (500 mL). The residue was suspended in THF and the mixture was refluxed for 12 h and filtered to give **4T-(chol)**, as a yellow solid (2.9 g, 2.1 mmol, 94%). M.p. 254 °C (decomp); <sup>1</sup>H NMR (600 MHz, 1,1,2,2-C<sub>2</sub>D<sub>2</sub>Cl<sub>4</sub>, 373 K): δ = 0.73 (s, 6H; CH<sub>3</sub>), 0.92–2.37 (m, 68H; CH, CH<sub>2</sub>, CH<sub>3</sub>), 3.43–3.44 (m, 4H; CH<sub>2</sub>), 3.56–3.57 (m, 4H; CH<sub>2</sub>), 4.51–4.52 (m, 2H; CH), 4.94 (brs, 2H; NH), 5.37–5.38 (m, 2H; CH), 6.58 (brs, 2H; NH), 7.16 (s, 4H; Ar), 7.20 (s, 2H; Ar), 7.44 ppm (s, 2H; Ar); ATR-IR: ν = 3347, 1696, 1630, 1533, 791 cm<sup>-1</sup>; MS (MALDI-TOF, matrix; dithranol): 1328.92 [M+H]<sup>+</sup> (calcd: 1328.99); UV/Vis (1,1,2,2-C<sub>2</sub>H<sub>2</sub>Cl<sub>4</sub>): λ<sub>max</sub> (ε) = 418 nm (38820 mol<sup>-1</sup>L cm<sup>-1</sup>); elemental analysis calcd (%) for C<sub>78</sub>H<sub>110</sub>N<sub>4</sub>O<sub>6</sub>S<sub>4</sub>·1.9CH<sub>3</sub>OH: C 69.10, H 8.53, N 4.03; found: C 68.96, H 8.34, N 4.16.

**Preparation of 5T-(chol)<sub>2</sub>:** This compound was prepared by using a similar procedure to that described for compound **4T-(chol)<sub>2</sub>** from **4** (2.0 g, 3.0 mmol) and **6** (1.2 g, 1.5 mmol) and obtained as an orange solid (0.81 g, 0.57 mmol, 38%). M.p. 238–239 °C; <sup>1</sup>H NMR (600 MHz, 1,1,2,2-C<sub>2</sub>D<sub>2</sub>Cl<sub>4</sub>, 373 K): δ = 0.73 (s, 6H; CH<sub>3</sub>), 0.92–2.37 (m, 68H; CH, CH<sub>2</sub>, CH<sub>3</sub>), 3.43–3.44 (m, 4H; CH<sub>2</sub>), 3.57–3.58 (m, 4H; CH<sub>2</sub>), 4.53–4.54 (m, 2H; CH), 4.93 (brs, 2H; NH), 5.38–5.39 (m, 2H; CH), 6.56 (brs, 2H; NH), 7.01–7.44 ppm (m, 10H; Ar); ATR-IR: ν = 3330, 1691, 1628, 1539, 791 cm<sup>-1</sup>; MS (MALDI-TOF, matrix; dithranol): 1409.51 [M+H]<sup>+</sup> (calcd: 1411.11); UV/Vis (1,1,2,2-C<sub>2</sub>H<sub>2</sub>Cl<sub>4</sub>): λ<sub>max</sub> (ε) = 424 nm (43430 mol<sup>-1</sup>L cm<sup>-1</sup>); elemental analysis calcd (%) for C<sub>82</sub>H<sub>112</sub>N<sub>4</sub>O<sub>6</sub>S<sub>5</sub>·0.55CHCl<sub>3</sub>: C 67.18, H 7.69, N 3.80; found: C 67.23, H 7.69, N 3.80.

**Preparation of 11:** This compound was prepared by using a similar procedure to that described for compound **4T-(chol)<sub>2</sub>** from **10** (3.1 g, 11 mmol). Compound **11** was obtained as a yellow solid (6.8 g, 9.1 mmol, 86%). M.p. 189–190 °C; <sup>1</sup>H NMR (600 MHz, CDCl<sub>3</sub>, 298 K): δ = 0.67 (s,

3H; CH<sub>3</sub>), 0.86–2.29 (m, 34H; CH, CH<sub>2</sub>, CH<sub>3</sub>), 3.42–3.43 (m, 2H; CH<sub>2</sub>), 3.52–3.56 (m, 2H; CH<sub>2</sub>), 4.47–4.51 (m, 1H; CH), 5.08–5.09 (m, 1H; NH), 5.31–5.32 (m, 1H; CH), 6.98–6.99 (m, 2H; Ar), 7.04 (d, *J* = 3.8 Hz, 1H; Ar), 7.10 (brs, 1H; NHCOO), 7.39 (d, *J* = 3.8 Hz, 1H; Ar); ATR-IR: ν = 3335, 1710, 1615, 1539, 750 cm<sup>-1</sup>; MS (MALDI-TOF, matrix; dithranol): 766.89 [M+Na]<sup>+</sup> (calcd: 767.41); elemental analysis calcd (%) for C<sub>39</sub>H<sub>53</sub>BrN<sub>2</sub>O<sub>3</sub>S<sub>2</sub>: C 62.97, H 7.45, N 3.77; found: C 62.94, H 7.46, N 3.77.

**Preparation of 6T-(chol)<sub>2</sub>:** This compound was prepared by using a similar procedure to that described for compound **4T-(chol)<sub>2</sub>** from **5** (1.5 g, 2.0 mmol) and **11** (3.0 g, 4.1 mmol) and obtained as a red solid (2.6 g, 1.7 mmol, 85%). M.p. 247 °C (decomp); <sup>1</sup>H NMR (600 MHz, 1,1,2,2-C<sub>2</sub>D<sub>2</sub>Cl<sub>4</sub>, 373 K): δ = 0.73 (s, 6H; CH<sub>3</sub>), 0.92–2.37 (m, 68H; CH, CH<sub>2</sub>, CH<sub>3</sub>), 3.44–3.46 (m, 4H; CH<sub>2</sub>), 3.57–3.58 (m, 4H; CH<sub>2</sub>), 4.52–4.53 (m, 2H; CH), 4.93 (brs, 2H; NH), 5.38–5.39 (m, 2H; CH), 6.55 (brs, 2H; NH), 7.07–7.44 ppm (m, 12H; Ar); ATR-IR: ν = 3354, 1692, 1627, 1537, 790 cm<sup>-1</sup>; UV/Vis (1,1,2,2-C<sub>2</sub>H<sub>2</sub>Cl<sub>4</sub>): λ<sub>max</sub> (ε) = 439 nm (26770 mol<sup>-1</sup>L cm<sup>-1</sup>); MS (MALDI-TOF, matrix; dithranol): 1493.78 [M+H]<sup>+</sup> (calcd: 1493.24); elemental analysis calcd (%) for C<sub>88</sub>H<sub>114</sub>N<sub>4</sub>O<sub>6</sub>S<sub>6</sub>·4H<sub>2</sub>O: C 66.54, H 7.74, N 3.53; found: C 66.75, H 7.67, N 3.56.

## Acknowledgements

We thank Ms. M. Fujita of Kyushu University for AFM measurements and Prof. Dr. H. Wariishi, Dr. T. Kitaoka, and A. Mayumi of Kyushu University for Raman measurements. This work was partially supported by Grant-in-Aid for Young Scientists (B) (No. 16750122) and the 21st Century COE Program, "Functional Innovation of Molecular Informatics" from the Ministry of Education, Culture, Sports and Technology of Japan and JSPS fellowships (for S.-i.K.).

- [1] For the recent reviews: a) M. Leclerc, *Adv. Mater.* **1999**, *11*, 1491–1498; b) R. D. McCullough, *Adv. Mater.* **1998**, *10*, 93–116.
- [2] a) G. Barbarella, M. Zambianchi, A. Bongini, L. Antolini, *Adv. Mater.* **1993**, *5*, 834–839; b) J.-H. Liao, M. Benz, E. LeGoff, M. Kanatjidiz, *Adv. Mater.* **1994**, *6*, 135–138; c) H. Mugeruma, T. K. Saito, S. Hotta, *Thin Solid Films* **2003**, *445*, 26–31.
- [3] For the recent reviews: a) P. Terech, R. G. Weiss, *Chem. Rev.* **1997**, *97*, 3133–3159; b) J. H. van Esch, B. L. Feringa, *Angew. Chem.* **2000**, *112*, 2351–2354; *Angew. Chem. Int. Ed.* **2000**, *39*, 2263–2266; c) O. Gronwald, S. Shinkai, *Chem. Eur. J.* **2001**, *7*, 4328–4334, and references therein; d) A. Ajayaghosh, S. J. George, V. K. Praveen, *Angew. Chem.* **2003**, *115*, 346–349; *Angew. Chem. Int. Ed.* **2003**, *42*, 332–335; e) S. J. George, A. Ajayaghosh, P. Jonkheijm, A. P. H. J. Schenning, E. W. Meijer, *Angew. Chem.* **2004**, *116*, 3504–3507; *Angew. Chem. Int. Ed.* **2004**, *43*, 3422–3425; f) Y. Iwashita, K. Sugiyasu, N. Fujita, S. Shinkai, *Chem. Lett.* **2004**, *33*, 1124–1125.
- [4] a) K. Sugiyasu, N. Fujita, S. Shinkai, *Angew. Chem.* **2004**, *116*, 1249–1253; *Angew. Chem. Int. Ed.* **2004**, *43*, 1229–1233; b) S.-i. Kawano, N. Fujita, S. Shinkai, *J. Am. Chem. Soc.* **2004**, *126*, 8592–8593.
- [5] a) L. Ping, T. Zhen, D. Wen-ji, *Gaodeng Xuexiao Huaxue Xuebao* **2002**, *23*, 1632–1637; b) B. W. Messmore, J. F. Hulvat, E. D. Sone, S. I. Stupp, *J. Am. Chem. Soc.* **2004**, *126*, 14452–14458; c) P. Liu, Y. Shiota, Y. Osada, *Polym. Adv. Technol.* **2000**, *11*, 512–517.
- [6] K. Tsuchiya, Y. Orihara, Y. Kondo, N. Yoshino, T. Ohkubo, H. Sakai, M. Abe, *J. Am. Chem. Soc.* **2004**, *126*, 12282–12283.
- [7] a) B. M. W. Langeveld-Voss, M. P. Christiaans, R. A. J. Janssen, E. W. Meijer, *Macromolecules* **1998**, *31*, 6702–6704; b) J. J. Apperloo, R. A. J. Janssen, P. R. L. Malenfant, J. M. J. Fréchet, *Macromolecules* **2000**, *33*, 7038–7043.
- [8] F. S. Schoonbeek, J. H. van Esch, B. Wegewijs, D. B. Rep, M. P. de Haas, T. M. Klapwijk, R. M. Kellogg, B. L. Feringa, *Angew. Chem.* **1999**, *111*, 1486–1490; *Angew. Chem. Int. Ed.* **1999**, *38*, 1393–1397.
- [9] T. Ishi-i, R. Iguchi, E. Snip, M. Ikeda, S. Shinkai, *Langmuir* **2001**, *17*, 5825–5833.

- [10] J. J. Apperloo, R. A. J. Janssen, P. R. L. Malenfant, L. Groenendaal, J. M. J. Fréchet, *J. Am. Chem. Soc.* **2000**, *122*, 7042–7051.
- [11] Y. Wei, B. Wang, W. Wang, J. Tian, *Tetrahedron Lett.* **1995**, *36*, 665–668.
- [12] B. S. Ong, Y. Wu, P. Liu, S. Gardner, *J. Am. Chem. Soc.* **2004**, *126*, 3378–3379.
- [13] The gel to sol phase-transition temperature ( $T_{\text{gel}}$ ) under these conditions is 32 °C. Note that the aggregate of **4T-(chol)**<sub>2</sub> is gradually dissociated when temperature is raised, but the aggregate still exists even above the  $T_{\text{gel}}$ .
- [14] a) M. A. Hempenius, B. M. W. Langeveld-Voss, J. A. E. H. van Haare, R. A. J. Janssen, S. S. Sheiko, J. P. Spatz, M. Möller, E. W. Meijer, *J. Am. Chem. Soc.* **1998**, *120*, 2798–2804; b) A. Yassar, G. Horowitz, P. Valatm V. Wintgens, M. Hmyene, F. Deloffre, P. Srivastava, P. Lang, F. Garnier, *J. Phys. Chem.* **1995**, *99*, 9155–9159.
- [15] B. M. W. Langeveld-Voss, R. J. M. Waterval, R. A. J. Janssen, E. W. Meijer, *Macromolecules* **1999**, *32*, 227–230.
- [16] These suggestions have been reported in some related papers; a) M. C. R. Delgado, J. Casado, V. Hernandez, J. T. L. Navarrete, G. FuHrmann, P. Bäuerle, *J. Phys. Chem. B* **2004**, *108*, 3158–3167; b) C. M. Castro, M. C. Delgado, V. Hernandez, S. Hotta, J. Casado, J. T. L. Navarrete, *J. Chem. Phys.* **2002**, *116*, 10419–10427.
- [17] a) N. Harada, S.-M. L. Chen, K. Nakanishi, *J. Am. Chem. Soc.* **1975**, *97*, 5345–5352; b) K. Murata, M. Aoki, T. Suzuki, T. Harada, H. Kawabata, T. Komori, F. Ohseto, K. Ueda, S. Shinkai, *J. Am. Chem. Soc.* **1994**, *116*, 6664–6676, and reference cited therein.
- [18] K. J. C. van Bommel, C. van der Pol, I. Muizebelt, A. Friggeri, A. Heeres, A. Meetsma, B. L. Feringa, J. van Esch, *Angew. Chem.* **2004**, *116*, 1695–1699; *Angew. Chem. Int. Ed.* **2004**, *43*, 1663–1667.
- [19] J. Guay, P. Kasai, A. Diaz, R. Wu, J. M. Tour, L. H. Dao, *Chem. Mater.* **1992**, *4*, 1097–1105.
- [20] R. B. Martin, *Chem. Rev.* **1996**, *96*, 3043–3064.
- [21] a) F. Würthner, C. Thalacker, S. Diele, C. Tschierske, *Chem. Eur. J.* **2001**, *7*, 2245–2253; b) F. Würthner, Z. Chen, F. J. M. Hoeben, P. Osswald, C.-C. You, P. Jonkheijm, J. v. Herrikhuizen, A. P. H. J. Schenning, P. P. A. M. van der Schoot, E. W. Meijer, E. H. A. Beckers, S. C. J. Meskers, R. A. J. Janssen, *J. Am. Chem. Soc.* **2004**, *126*, 10611–10618.

Received: March 10, 2005

Published online: May 24, 2005